C.P. PANG
J.T. LUE[✉]

Monte Carlo simulation and optical transmission studies of lattice-tunable column arrays composed of ferrofluids

Department of Physics, National Tsing-Hua University, Hsin Chu, Taiwan

ABSTRACT The aggregation and rearrangement of nanoparticles embedded in a thin cell of ferrofluid at various applied magnetic fields was studied by Monte Carlo simulation. Regular microcolumns with the axis parallel to the magnetic field were observed with column size and spacing depending on the ramp speed of the applied field. Our model successfully simulated the reported experimental results that the column size decreases as the ramp speed increases, which is attributed to the diminishing time to achieve the final assembled state at a given final magnetic field. Column arrays of tunable lattice constants characterizing various spectroscopic dispersions are elucidated. The hexagonal structure of the aggregation of magnetic nanoparticles and optical dispersion were observed through an optical microscope. The transmission diffraction spectra depending on column spacings and sizes of the column array are simulated to yield results comparable to the experiment.

PACS 75.50.Mm; 75.75.+a; 42.25.Hz

1 Introduction

Ferrofluids are composed of small single-domain magnetic nanoparticles that are dispersed in a non-magnetic fluid. The small nanoparticles, covered with surfactant to prevent clumping together on account of the repulsive van der Waals force (which is attractive at far separation), are kept randomly dispersed through the fluid due to the Brownian motion at room temperature without applying external magnetic fields. Photonic crystals inheriting a periodic lattice structure exhibit a band gap that forbids light propagation over a certain frequency range [1–3]. This property enables one to manipulate light propagation with amazing facility and produces effects that are inaccessible by conventional optics [4]. Recently, many reports concerning the applications and theoretical calculations of photonic crystals have been published extensively[1]. Among these works, the lattice-tunable photonic crystals suggest a controllable photonic band gap through external magnetic fields and generate attention for more germane applications in optical devices [5–8]. The

column arrays constructed by ferrofluids under an applied external ramp field can have similar optical properties to a photonic crystal in two dimensions (2-D) but with tunable lattice constants. To study optical properties such as transmittance and reflectance of a 2-D photonic crystal, light should be directed parallel to the plane. For opaque columns formed in a thin magnetic fluid film ($\sim 10\,\mu m$), it will be much easier if the crystalline structure is analyzed by examining the transmittance pattern with light perpendicular to the cell plane. This work concentrates on the numerical calculation of column sizes and spacings between magnetic particles dispersed in ferrofluids, and the examination of the spectroscopic dispersion incorporation with a microscope.

That polyethylene microspheres of 1–10 μm in diameter dispersed in ferrofluid are rearranged into a regular lattice as an external magnetic field is applied was well known for a long time. In this work, we attempt to introduce a time-dependent magnetic field perpendicular to the thin magnetic fluid film, by which the embedded nanoparticles start to agglomerate and form columns along the direction of the field [9–11]. In thermal equilibrium, these microcolumns arrange in a structure of a hexagonal lattice to minimize the free energy of the system [12]. The experimental result showed that the size of the magnetic columns is effectively tuned by varying the ramp speed of the magnetic field [13]. The total magnetic moment of each microcolumn changes depending on the size of the column. Besides, the effect of magnetic permeability, which has been neglected in many works in theoretical calculation of photonic crystals, is discussed in this work.

The main aim of this paper is, by using Monte Carlo (MC) simulation, to understand how the ramp speed of the applied magnetic field determines the sizes of the aggregated microparticles and the regular spaces between the columns. Secondly, we propose a computational method for analyzing the transmission color distribution of an imperfect hexagonal lattice to confirm the same spectrum resulting either from the interference of point sources of opaque columns or from spaces between columns.

2 Magnetic nanoparticles in ferrofluids and Monte Carlo simulation

Magnetite nanoparticles were prepared by a co-precipitation method that has been conventionally

[✉] Fax: +886-35723052, E-mail: jtlue@phys.nthu.edu.tw
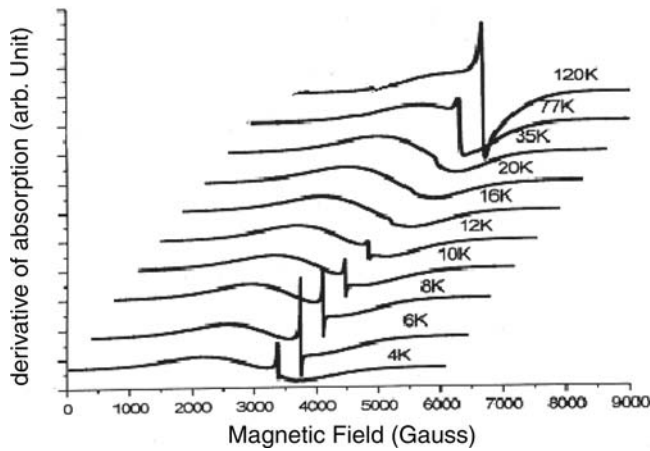
[1] http://home.earthlink.net/~jpdowling/pbgbib.html

FIGURE 1 The ESR spectra for Fe_3O_4 ferrofluid measured at various temperatures from 4 K to 220 K. Since our system can only go down to 4 K, we include the *inset* to adduce the approaching of a constant intensity below the critical temperature for the much smaller particles that have a higher critical temperature

FIGURE 3 A schematic drawing of the lattice at the center of mass of transparent spaces between the opaque hexagonal columns

implemented to produce ferrofluids [14]. The thermally fluctuating magnetization directions of the monodomain magnetic nanoparticles are illustrated to be in superparamagnetic state at room temperature. As the temperature decreases, the thermal fluctuation of the magnetic moments is blocked and the exchange interaction between neighboring nanoparticles is high enough to align their spins. The conversion of ferromagnets to quantum superparamagnets in anisotropic ferromagnetic nanoparticles becomes saliently due to quantum tunneling on applying a transverse microwave magnetic field or implicitly by an internal anisotropic field perpendicular to the easy axis at low temperatures. The spectral line width observed by an electron spin resonance (ESR) spectrometer as shown in Fig. 1 [15] clearly expresses this phase change as the temperature decreases. The retained superparamagnetic state in a strong static magnetic field clearly portrays the absence of exchange interaction between neighboring nanoparticles with particle surfaces covered with surfactant. This fact suggests that we should consider only the dipole–dipole interactions between particles in this simulation. Column arrays of tunable lattice constants characterizing various spectroscopic dispersions are elucidated. The simulated spectral distributions successfully agree with the interference dispersion of grating slits as prescribed by this Monte Carlo simulation.
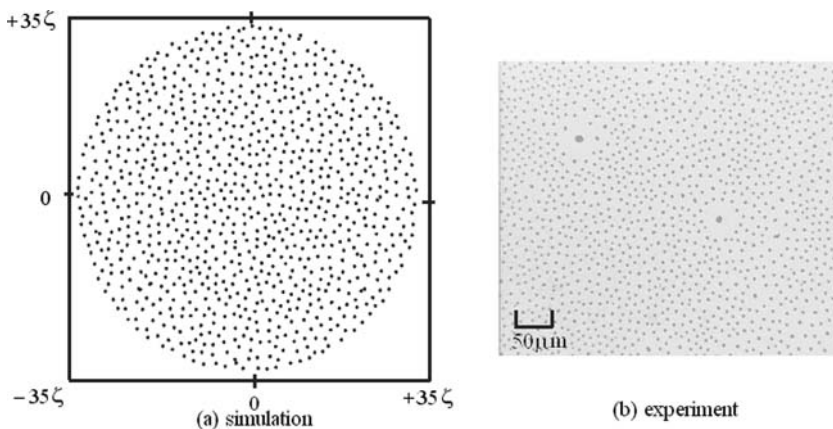
The ferrofluid of nanometer size appears transparent. The dispersed magnetic nanoparticles aggregate to form clusters or columns as an external ramped magnetic field is applied, resulting from achieving the thermal equilibrium state. At constant temperature and density, the minimizing of free energy can be replaced by the minimizing of internal energy. A quasi-hexagonal lattice structure far from a perfect crystal can be observed, as shown in Fig. 2b. The regular lattice points formed by the aggregation of nanomagnetic particles are displayed resulting from an external ramped magnetic field.

For analyzing such an imperfect structure, Fourier transformation and a grating model were exploited [13]. The Fourier transformation expresses the dispersed wave vectors from the space distribution among magnetic columns but it is impractical to know the positions of each column in advance, whereas the grating model is valid only when the column sizes are much smaller than the spacing between neighboring columns. Practically, for a dense or a thick film, the transmitted light passing through narrow slits displays interference owing to the large coverage of opaque columns. As shown in Fig. 3, the centers of slits between opaque columns composing a hexagonal lattice are illustrated as effective lattices that differ from the original hexagonal structure. In analyzing the crystalline structure formed in ferrofluids by

FIGURE 2 **a** A snapshot of the simulated 1000 columns (of size ζ) with an out-of-plane field after 10 000 MC steps. **b** The regular lattice points formed by the aggregation of nanomagnetic particles resulting from an external ramped magnetic field
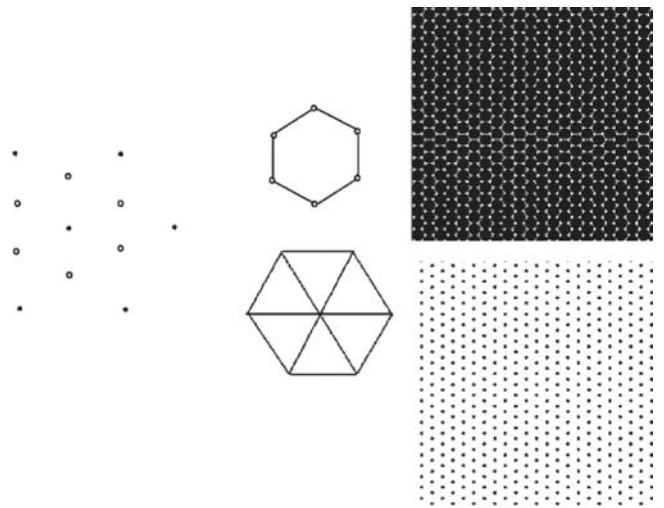
the transmittance pattern, this divergence of light should be considered.

Magnetic nanoparticles dispersed in ferrofluids are of nanometer size, while the magnetic columns formed after applying an external magnetic field are of micrometer size both in diameter and in length. There are approximately 10^{6-7} nanoparticles in a single column, which are difficult to manipulate even by present supercomputers. To save the time consumption in computation for the simulation of the aggregation of magnetic particles, we largely reduce the number of particles while retaining the physical framework.

The whole system can be divided equally into sub-cells with the magnetic moment of each cell remaining at zero. In this model, each cell of the ferrofluid is mimicked as a single magnetic particle, called a modeled magnetic particle (MMP), with a magnetic moment M_{MMP} that is linearly proportional to the strength of the applied field, i.e. $M_{MMP} \propto H_z$.

The thermodynamic equilibrium of the magnetic fluid under an applied magnetic field at temperature T implies the free energy

$$F = U - TS \tag{1}$$

to be a minimum, where U is the internal energy and S is the entropy associated with the translational degrees of freedom of this system as approximated [16, 17] by

$$S = Nk \ln \left(\frac{\Omega}{\lambda^3} \right), \tag{2}$$

in which N is the total MMP number, Ω the sample volume depending on the aggregation of the nanoparticles and λ the thermal wavelength of the MMPs depending on the temperature T and the density ρ. Considering T and ρ to be constants, and the change of Ω to be negligibly small, the minimizing of the free energy can be replaced by the minimizing of U.

The MMPs are specified by their center positions and magnetizations. The dipole–dipole interaction energy between neighboring particles has two components: (i) the interaction energy with Hamiltonian $H = \sum_{ij} V_{ij}$, where

$$V_{ij} = A \left\{ \left[\frac{\sigma}{\| \bar{r}_j - \bar{r}_i \|} \right]^{12} - \left[\frac{\sigma}{\| \bar{r}_j - \bar{r}_i \|} \right]^6 \right\} \tag{3}$$

is the Lennard–Jones potential in which A is a constant specifying the interaction intensity between particles within a hard core of grain diameter σ. Short-range interactions such as the attractive van der Waals force and the repulsive force resulting in the overlapping electron orbits are already considered in the Lennard–Jones potential, which represents the strength where these two forces are balanced. The second component is (ii) the magnetic dipole–dipole interaction energy:

$$H_{dip} = B \sum_{ij} \left(\frac{\bar{M}_i \cdot \bar{M}_j}{r_{ij}^3} - 3 \frac{(\bar{M}_i \cdot \bar{r}_{ij})(\bar{M}_j \cdot \bar{r}_{ij})}{r_{ij}^5} \right). \tag{4}$$

Here B is a dipole-coupling constant with an energy unit of B/σ^3 and M_i is the magnetization of the ith MMP that is proportional to the applied magnetic field at each time step. The linear time variation of the magnetic field is approached by the step change in this Monte Carlo simulation. The quasi-thermal equilibrium at each time-step simulation is established, as the

time variation of the magnetic field is slow enough for the nanoparticles to migrate to their equilibrium positions. This time-step simulation is justified by the experimental observation as shown in Fig. 2. With an applied external magnetic field $\bar{H}$, the Zeeman interaction is

$$H_{Ze} = -\sum_i \bar{H}_z \cdot \bar{M}_i. \tag{5}$$

In fact, ferrofluids are colloidal dispersions of magnetic monodomain nanoparticles in a carrier liquid. MC simulation of the effects of colloidal properties such as polydispersity was reported recently [18, 19]. For our modeled magnetic particles, we simply consider the system to be a monodisperse and purely dipolar system, i.e. equally sized particles with a repulsive core. The Brownian motion resulting in diffusing particles occurring in gas and liquid is involved in the simulation during the random movement of MMPs with specified range and orientation, with negligible values in the concentrated ferrofluids in comparison to the magnetic dipole–dipole field during the application of the external field. The rotational energy is much smaller than the translation energy of the nanoparticles. We can consider the magnetization energy U, which includes only the above three interaction energies. The Monte Carlo simulation starts from a uniform distribution of MMPs within a rectangular volume of $10 \times 10 \times 5\sigma^3$ inheriting randomly oriented magnetic moments. We define the probability p which determines the computation of each Monte Carlo step (MCS) to be terminated when p is either greater than or equal to a randomly generated variable b, which lies between 0 and 1. The probability $p = 1$ for $\Delta U < 0$ and or $p = e^{-\Delta U / kT}$ for $\Delta U > 0$. If p is smaller than b, the nanoparticle is kept at its old position; otherwise it will change to a new position to continue the MCS. The configurations are regulated by a random spatial excursion within a sphere of radius $\alpha\sigma$ with $0 < \alpha < 1$, and a random orientation of the magnetization moment for the unit sphere. They are relaxed according to the Monte Carlo process at the temperature $T = 0.1/k_B$ expressed in a dipolar energy unit. This temperature was chosen to allow spin and displacement variations small enough to maintain the magnetic interaction, but large enough to ensure relaxation [20]. The constraint of Monte Carlo steps occurs when the displacement extrudes the rectangular cell.

3   Coherent point sources for column arrays

It is generally attempted to simulate the optical interference pattern from the ordered arrangement of rods in ferrofluids. This is anticipated by taking each column as a coherent light source if the column size is small enough to be considered as the center of diffraction as shown in Fig. 4, where the interference for the light at wavelength λ occurs at the screen at a distance L. Each diffraction spot on the screen is the sum of the irradiations from each point of the sample. Each point contributes an amount of field $|e^{i\phi}|/L_\lambda$, where L_λ is the light path and $\phi = 2\pi L_\lambda / \lambda$ is the angular phase shift. The contribution of the diffracted field is inversely proportional to the optical path.

As the column size increases to about the spacing between columns, it is more germane to take the center of mass of any
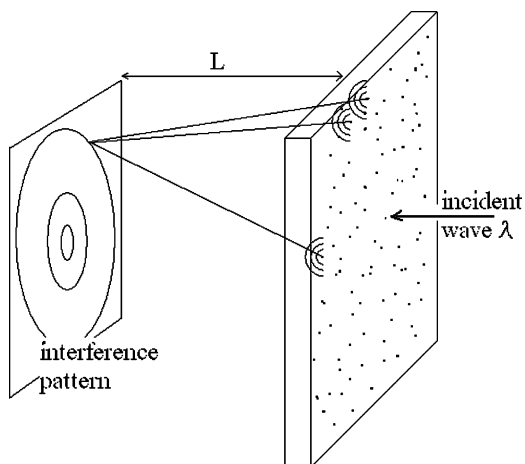
FIGURE 4   The coherent point-source model with the resolution of the screen L set at 200×200. The interference intensity is calculated by summing over the contributions from each point

three adjacent columns to be the light source, as shown in Fig. 3. The center of mass can be effectively specified by an algorithm exploited in this programming [21]. The procedures are:

1. Making lines for any two points and denoting them as line pools A.
2. Sorting the A lines with respect to their lengths with an increment.
3. Creating a new pool B.
4. Copying the shortest A line to pool B where it does not cross any line in B (except at vertices).
5. Removing the shortest A line.
6. Repeating procedures 4 and 5 until exhausting the A lines.
7. Identifying the center of mass for any triangle formed by three lines in B.

4   Results and discussion

To illustrate the effect of the ramp speed of external fields on the aggregations of magnetic nanoparticles in ferrofluids, all parameters in this Monte Carlo simulation are predetermined except for the magnitudes of the fields that vary with the simulation steps. The results of the three-dimensional (3-D) configuration for the sample with 500 MMPs after 1000 MC steps subjected to an external field increasing step by step of $H_z = steps\ /\ MCS$ are shown in Fig. 5. The MMPs, firstly, aggregated into micrometer particles and then formed regular columns aligning parallel to the applied magnetic field after 1000 Monte Carlo steps (MCS) with a maximum field $H_z = 1$. For a 500-MMP system, the 1000 MCS took $500 \times (500 - 1) \times 1000$ computing cycles ($\sim O(N^2)$) to complete the simulation. The simulating is furnished for different $H_z = (steps \times R)\ /\ MCS$ by varying the ramp rate R of the applied field. Physically, ferrofluids are relaxed to become dispersed after each ramp field. Figure 6 shows the top view of several simulated configurations for increasing R at speeds of 1, 2, 3, 4 and 5, respectively. It reveals that the faster the ramp rate, the higher the density of the columns with the smaller size of each column. This
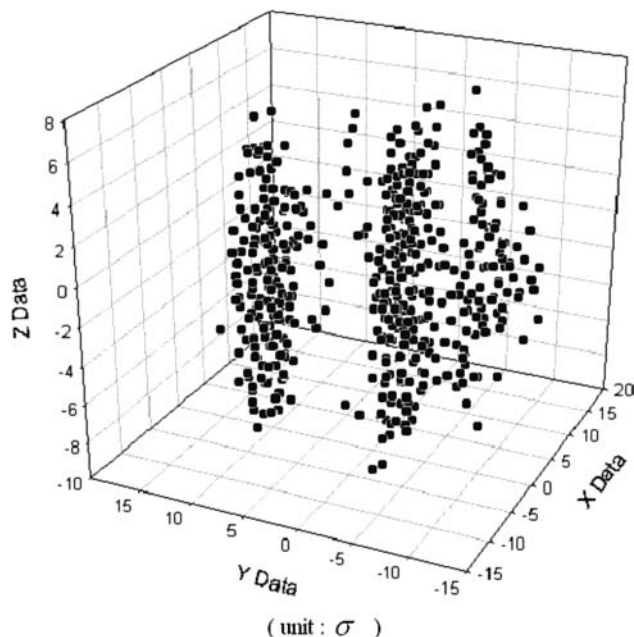

FIGURE 5   A 3-D snapshot of 500 MMPs after 1000 MC steps

evidence can be portrayed that the faster the time for nanoparticles to achieve their final assembled state at a given final magnetic field, the fewer the particles that are involved in this migration. As indicated in Fig. 6, which shows snapshots of 500 MMPs with an out-of-plane field after 1000 MC steps with different ramping rates, the decrease of total magnetic moment in each column results in a decrease of lattice constants embodied in a magnetic repulsive force. We have evaluated
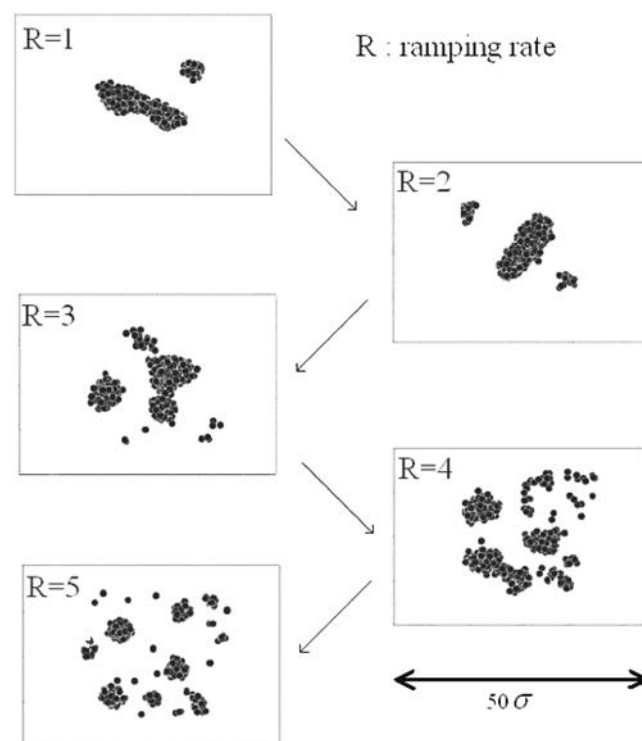

FIGURE 6   Snapshots of 500 MMPs with an out-of-plane field after 1000 MC steps with different ramping rates
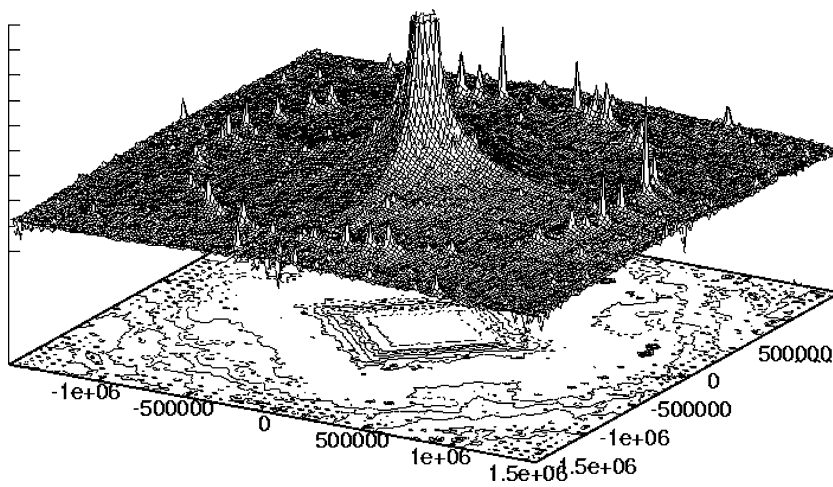
the lattice constants for the quasi-hexagonal crystalline structure of ferrofluids by tedious Monte Carlo simulations. For a particular density of ferrofluids used in this simulation, the number of MMPs in a specified volume is given by $V = A \times height$; the more the columns formed at a higher ramping rate of the magnetic field, the shorter the lattice constants. The distance d between two agglomerates is given, on average, by

$$d^2 = \frac{4A}{\sqrt{3}N_t} \propto \frac{1}{N_c}, \qquad (6)$$

where N_t is the number of triangles formed by three adjoining columns, which is proportional to the number of agglomerates N_c.

Exploiting this simulated hexagonal lattice as shown in Fig. 2a, we can establish the interference patterns in 3D and 2D as shown, respectively, in Figs. 7 and 8 through the assumption of a coherent point light source. Here, we assume that L and λ are 1×10^5 and 0.5, respectively, and that the

resolution of the interference screen is 200×200. The color histogram represents the contour of the same interference intensity with the zero order located at the center.

The simulated interference angle $\theta_s^1 (\cong r_s/L)$ is adjusted to be equal to that of the experimental value by varying λ_s, the wavelength in the simulation. Then, the experimental column distance d_{exp} in ferrofluids is given by $(\lambda_{exp}/\lambda_s)d_s$, where d_s is the parameter of the column distance in this simulation, which can be set as unity. It is worth noting that what we have done is not using the controversial grating model to determine d_{exp} but using the analogous simulation of interferences with the estimated d_{exp}. In this sense, we normalize the quantities used in the simulation and then scale them to match the experimental result.

For a more dense fluid with the light transmission very small, it is better to take the slits between magnetic columns as the new light source as indicated as the center of mass in the triangular points as given in Fig. 3. The simulated spectral contour with the same λ_s, θ_c^1 and L is shown in Fig. 9. The
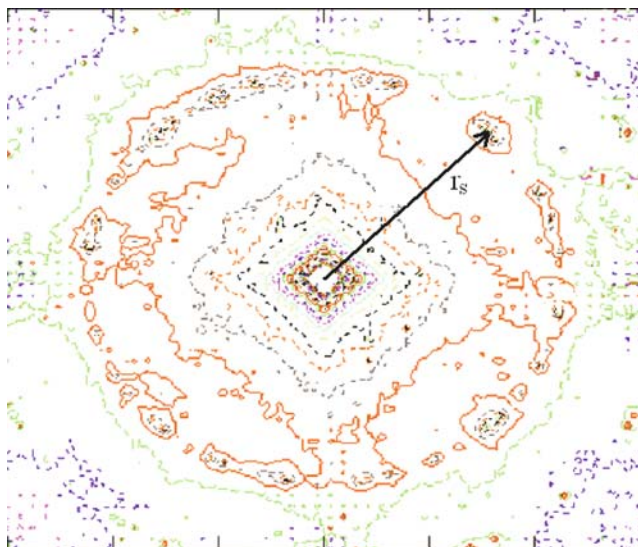

FIGURE 8   Histogram showing the contours of interference intensity using the points in Fig. 2a as the coherent light sources
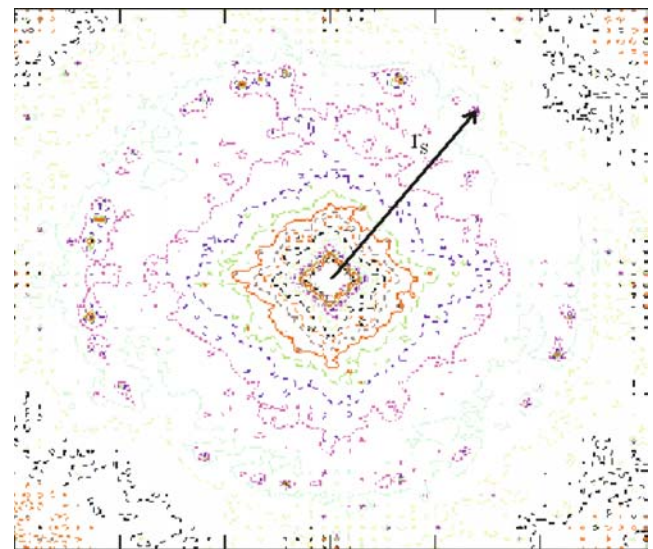

FIGURE 9   Histogram showing contours of interference intensity using the centers of mass of triangular spaces of point sources in Fig. 2a as the coherent light sources
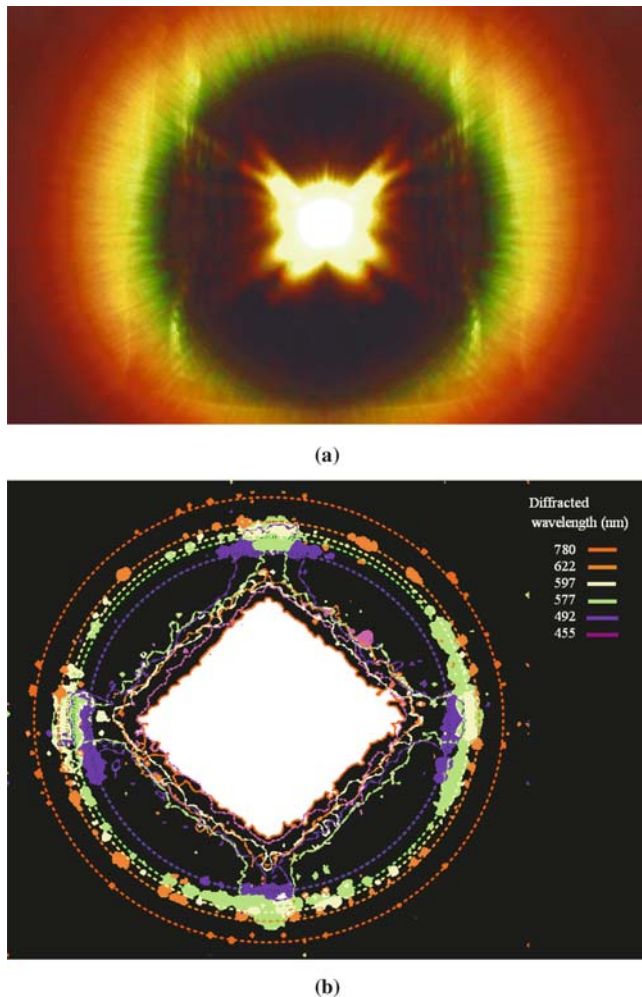
(a)

(b)

FIGURE 10 **a** Experimental transmittance pattern with incident white light. The ferrofluid used kerosene-based Fe_3O_4 magnetic nanoparticles with oleic acid as surfactant. The thickness of the cell was 10 μm. The ramping rate of the field was 5 Oe/s and fixed at 600 Oe for equilibrium. **b** Simulated transmittance pattern with various wavelengths using the points in Fig. 2a as the coherent light sources (with 1000 point sources)

results of the simulated spectral distributions by implementing the light source as emanating from the grating slits and from the magnetic columns are the same. We have plotted the contours for the spectral distribution of white light that was transmitted through the Monte Carlo simulated lattice for ferrofluids as shown in Fig. 2a. Experimental and simulated transmittance patterns with white light illuminating a ferrofluid are shown in Fig. 10a and b, respectively, which clearly reveal diffracted circles. There are some unexpectedly strong diffraction spots in the simulated pattern, which is due to the limited number of point sources (1000) in this simulation.

5   Conclusion

This Monte Carlo simulation illustrates that the magnetic nanoparticles embedded in ferrofluids aggregated into columns of microparticles with the particle size crucially inversely proportional to the ramp of the applied magnetic field. The spacing of the regular magnetic columns is also controlled by the ramp of the applied field, implying a tunable lattice for column arrays with the axis being parallel to the external field. With the simulated lattice we can numerically evolve the transmission spectra of the column array constructed by this ferrofluid. With this computation we can even draw the spectral contour for a non-perfect crystalline structure. This method is helpful in analyzing crystalline structures, especially for opaque agglomerations in thin ferrofluid cells exploited in 2-D photonic crystals.

REFERENCES

1 E. Yablonovitch, Phys. Rev. Lett. **58**, 2059 (1987)
2 S. John, Phys. Rev. Lett. **58**, 2486 (1987)
3 J.D. Joannopoulos, R.D. Meade, J.N. Winn, *Photonic Crystals: Molding the Flow of Light* (Princeton University Press, Princeton, NJ, 1995)
4 J.D. Joannopoulos, P.R. Villeneuve, S. Fan, Nature **386**, 143 (1997)
5 A. Figotin, Y.A. Godin, I. Vitebsky, Phys. Rev. B **57**, 2841 (1998)
6 I.L. Lyubchanskii, N.N. Dadoenkova, M.I. Lyubchanskii, E. Shapovalov, T. Rasing, A. Lakhtakia, A. Lakhtakia, G. Dewar, M.W. McCall, Proc. SPIE **4806**, 302 (2002)
7 C. Xu, X.H. Hu, Y.H. Li, X.H. Liu, R.T. Fu, J. Zi, Phys. Rev. B **68**, 193 201 (2003)
8 S.Y. Yang, H.E. Hong, C.H. Hong, H.C. Yang, M.C. Chou, C.T. Pan, Y.H. Chao, J. Appl. Phys. **93**, 3457 (2003)
9 N. Inaba, H. Miyajima, H. Takahashi, S. Taketomi, S. Chikazumi, IEEE Trans. Magn. **25**, 3866 (1989)
10 P. Pang, C.T. Hsieh, J.T. Lue, J. Phys. D: Appl. Phys. **36**, 1764 (2003)
11 T. Kruse, H.G. Krauthäuser, A. Spanoudaki, R. Pelster, Phys. Rev. B **67**, 094206 (2003)
12 C.Y. Hong, I.J. Jang, H.E. Hong, C.J. Hsu, Y.D. Yao, H.C. Yang, J. Appl. Phys. **81**, 4275 (1997)
13 C.Y. Hong, H.E. Hong, I.J. Jang, J.M. Wu, S.L. Lee, W.B. Yeung, H.C. Yang, J. Appl. Phys. **83**, 6771 (1998)
14 C.T. Hsieh, J.T. Lue, Phys. Lett. A **300**, 636 (2002)
15 C.T. Hsieh, J.T. Lue, Phys. Lett. A **316**, 329 (2003)
16 J.G. Kirkwood, J. Chem. Phys. **18**, 380 (1950)
17 J.O. Hirschfelder, C.F. Curtiss, R.B. Bird, in *Molecular Theory of Gases and Liquids* (Wiley, New York, 1954), p. 272
18 T. Kruse, A. Spanoudaki, R. Pelster, Phys. Rev. B **68**, 054208 (2003)
19 T. Kristóf, I. Szalai, Phys. Rev. E **68**, 041109 (2003)
20 A. Ghazali, J.-C. Lévy, Phys. Rev. B **67**, 064409 (2003)
21 F.P. Preparata, M.L. Shamos, *Computational Geometry: An Introduction* (Springer, Berlin Heidelberg New York, 1985)